



# 3D imaging of bean seeds: Correlations between hilum region structures and hydration kinetics

Laura Gargiulo, Giuseppe Sorrentino, Giacomo Mele\*

Institute for Agricultural and Forest Systems in the Mediterranean (ISAFoM), Department of Biology, Agriculture and Food Sciences (DiSBA), National Research Council (CNR), Italy

## ARTICLE INFO

### Keywords:

X-ray microCT  
Common bean landraces  
Water uptake  
Micropyle  
Bean morphometry

## ABSTRACT

X-ray micro-CT imaging has been applied successfully in food science and seed research due to its capacity to provide very small details of seed traits that are very complex to score. The micropyle and the tissues of the hilum region of bean seeds are recognized as structures which play an important role in hydration process. This latter influences, in turn, not only germination but also the cooking and industrial processing. Nevertheless, the role of each structure of the bean seeds is yet to be fully understood. Moreover such traits are never been quantified by using 3D imaging approaches.

In this work, seeds of four ancient Italian landraces of beans have been scanned by X-ray microCT with a twofold approach: bulk scans for whole seed imaging and single seed scans for internal traits measurements. Then water uptake tests have been performed. The different structures composing the hilum region of the beans have been imaged and characterized. The two-dimensional and the three-dimensional morphometric traits have been correlated with parameters of hydration models by Principal Component Analysis (PCA) and Pearson coefficients.

Micropyle groove area was the trait most influencing the very initial hydration rates while the hilum groove area was the best correlated with the overall infiltration behavior. The internal free space was the trait best correlated with the moisture at equilibrium. Moreover, strophiole shape resulted the most suitable internal trait for univocal identification of the four landraces.

Overall results give a contribution to the understanding of the role of hilum region structures in bean seeds hydration process and show novel morphological traits useful for identification of local bean landraces.

## 1. Introduction

Common beans (*Phaseolus vulgaris* L.) are one of the most important source of human dietary protein (Kotue et al., 2018). Most of their production volumes comes from landraces cultivated in traditional farming systems (Chávez-Servia et al., 2016) and represents local specialties with great economical potential (Veteläinen, 2009). Taste, high nutritional value, thin coat, short cooking time and good yield are among the most appreciated quality characteristics for such products (Piergiovanni & Lioi, 2010). Phenotyping based on seed image analysis is increasingly used as less expensive approach than molecular one in order to trace and authenticate bean landraces (e.g., Lo Bianco, Grillo, Cremonini, Sarigu, & Venora, 2015). Hydration behavior also contributes to define the overall quality of the bean landraces as the hydration process of pulses is a crucial step before cooking, germination, extraction, malting and fermenting (Miano & Augusto, 2018).

The hydration of grains before cooking helps to soften the bean structure, reduces the cooking time (Martínez-Manrique et al., 2011), enhances the heat transfer through the grain and improves the inactivation of anti-nutritional factors as tannins, phytic acid and oligosaccharides (Khattab & Arntfiel, 2009).

The contribution of different parts of the bean to the hydration process has been evaluated by alternatively covering (waterproofing) seed coat or hilum (Miano, Pereira, Castanha, Júnior, & Augusto, 2016) and by using MRI (Kikuchi, Koizumi, Ishida, & Kano, 2006), which allows to observe the hydration pathway during the soaking. Strophiole (Kikuchi et al., 2006), hilum and micropyle have been recognized as main initial entry points for water (Miano et al., 2016; Mikac, Sepe, & Serša, 2015; Agbo, Hosfield, Uebersax, & Klomparens, 1987), being the seed coat completely or partially impermeable, initially.

However, the hydration is a complex process involving all intrinsic physical characteristics of legume grains. Indeed, different aspects of

\* Corresponding author.

E-mail address: [giacomo.mele@cnr.it](mailto:giacomo.mele@cnr.it) (G. Mele).

<https://doi.org/10.1016/j.foodres.2020.109211>

Received 4 December 2019; Received in revised form 12 March 2020; Accepted 30 March 2020

Available online 06 April 2020

0963-9969/© 2020 Elsevier Ltd. All rights reserved.

hydration have been studied, such as characterizing different kinetics behavior and looking for innovative technologies to accelerate it.

Despite that, more studies need to be conducted to fully understand the role of each bean structure in the water uptaking behavior (Miano & Augusto, 2018), as well as the correlation between the grain structures and hydration characteristics (hydration rate, equilibrium moisture content and lag phase time). Until now only the scanning electron microscopy (SEM) has been used for the observation of these seed structures (Miano, Saldaña, Campestrini, Chiorato, & Augusto, 2018) and highlighted the genotypic variability of their characteristics (Berrios, Swanson, & Cheong, 1998; Agbo et al., 1987).

Nowadays X-ray microCT is successfully used in food science and seed research (Gargiulo, Grimberg, Repo-Carrasco-Valencia, Carlsson, & Mele, 2019; Gomes & Van Duijn, 2017; Schoeman, Williams, du Plessis, & Manley, 2016; Guelpa, du Plessis, & Manley, 2016; Gustin et al., 2013), because such technique allows to non-destructively and non-invasively visualize and characterize external and internal microstructure of small objects in three dimensions. However, to the best of our knowledge, morphometric characteristics of beans and, in particular, the structures of the hilum region have never been quantified by X-ray microCT imaging.

In this work X-ray microCT and image analysis procedures were performed for 3D morphometric characterization of four Italian bean landraces and their hilum region parts. Then bean hydration curves have been achieved. The aim was to correlate two dimensional and three-dimensional morphometry data of the grain structures with the parameters of the hydration model.

## 2. Materials and methods

### 2.1. Bean grains

Four Italian landraces of beans (*Phaseolus vulgaris* L.) produced in Campania Region (southern Italy) were used in the study. Butirro from Sorrento, Mustacciello from S. Antonio Abate and Zampognaro from Ischia were provided by the non-profit organization Slow Food, Convivium of Campania Region, while Quarantino from Volturara Irpina was provided by the local company Petretta Maria S.r.l.

These landraces are cultivated on very small areas (< 1 ha) and with limited production by custodian farmers who, thanks to regional funding and the promotion of Slow Food Campania, avoided their extinction, preserving the biodiversity of one of the richest Italian Region for plant biodiversity. Siano et al. (2018) have already characterized such bean landraces from a nutritional point of view. Quarantino from Volturara Irpina and Mustacciello are included in the list of traditional agri-food products held by the Italian Ministry of Agriculture Food and Forestry Policies,<sup>1</sup> while Butirro and Zampognaro are included in Slow Food “Arca del gusto” list.<sup>2,3</sup> Quarantino from Volturara Irpina is also a Slow Food presidium.<sup>4</sup>

### 2.2. X-ray microCT

The X-ray microCT scanning was performed using the microtomograph Bruker Skyscan 1272 available at the National Research Council of Italy - Institute for Agriculture and Forestry in the Mediterranean, Ercolano (Italy). It is a desktop microtomograph with a

cone beam X-ray source adjustable in the 20–100 kV energy range and allows as maximum sample size a cylinder shaped volume of 6.5 cm in diameter and 7.2 cm height.

As there are no standard procedures for seed micro CT scanning and analysis, multiple scanning and image analysis tests were performed trying different settings before reaching the final setup for the two scanning and analysis protocols described below.

#### 2.2.1. Bulk seed scanning

For the X-ray microCT scanning, about 70 seeds for each landrace were randomly selected and were acquired in one time arranging them in a poly-methyl methacrylate (PMMA) cylinder of 6 cm diameter whose internal surface was coated with a polystyrene film. The cylinder was 6.5 cm height and contained five or six superimposed polystyrene circular grids containing till thirteen seeds each. Such arrangement allowed the reconstruction and the analysis of 66 till 74 beans from a single scan, depending on the landrace seed size. PMMA material for the cylinder and the polystyrene for the grids were chosen because of their low X-ray attenuation capacity, allowing good contrast in the imaging of the seeds. The main function of the grids was to obtain an image where seeds did not touch each other, thus simplifying the following stage of image processing. Image acquisition was set at a source voltage and current of 50 kV and 200  $\mu$ A, respectively. X-ray scans were acquired at 20  $\mu$ m voxel size and required approximately 3.5 h to complete.

#### 2.2.2. Single seed scanning

For the characterization of the internal structures of the hilum region of each bean, a single scan for one seed at a time was performed.

The seeds were held on a very thin support using dental wax and put on the rotating stage of the microtomograph. In particular a sub-volume of each grain was acquired focusing the detector camera of the microtomograph on the hilum region of the bean.

Source voltage and current were set at 50 kV and 200  $\mu$ A, respectively, as above but with different geometric magnification and detector camera binning, obtaining images at 2  $\mu$ m voxel size. Each scan took approximately 2 h and 20 min to complete. Three seeds for each landrace were scanned.

### 2.3. Image processing

The series of two-dimensional X-ray projection images obtained from the micro-CT scans were reconstructed in a 3D image using the NRecon software, version 1.7.3.<sup>5</sup> The reconstruction procedure comprised a filtered back projection algorithm (Xiao, Bresler, & Munson, 2003). In order to obtain a proper 3D reconstruction of the images ring artifact and beam hardening corrections were applied at 18% and 70% level for the bulk seed scans and at 20% and 50% levels for the single seed scans, respectively.

The images were binarized applying different thresholds to the gray level histograms in order to segment each seed part using the CTAn software. In particular, images from the bulk seed scans were segmented to provide the whole grains and their internal free space, while the different structures of the hilum region (funicular tissue, vascular tissue, tracheid bars, strophiole and micropyle) were segmented on images from the single seed scans. In Figure 1 examples of reconstructed sections of the segmented seed parts are shown.

### 2.4. Image analysis

The segmented images were used to measure volumetric and morphological characteristics of the whole seed and of the tissues of the hilum region.

<sup>1</sup> <http://www.politicheagricole.it/flex/cm/pages/ServeBLOB.php/L/IT/IDPagina/3276>.

<sup>2</sup> <https://www.fondazioneSlowFood.com/it/arca-del-gusto-slow-food/fagiolo-butirro-di-vicoequense/>.

<sup>3</sup> <https://www.fondazioneSlowFood.com/it/arca-del-gusto-slow-food/fagiolo-zampognaro/>.

<sup>4</sup> <https://www.fondazioneSlowFood.com/it/nazioni-presidi/italia-it/?fwppaged=11>

<sup>5</sup> <http://www.bruker-microct.com>.

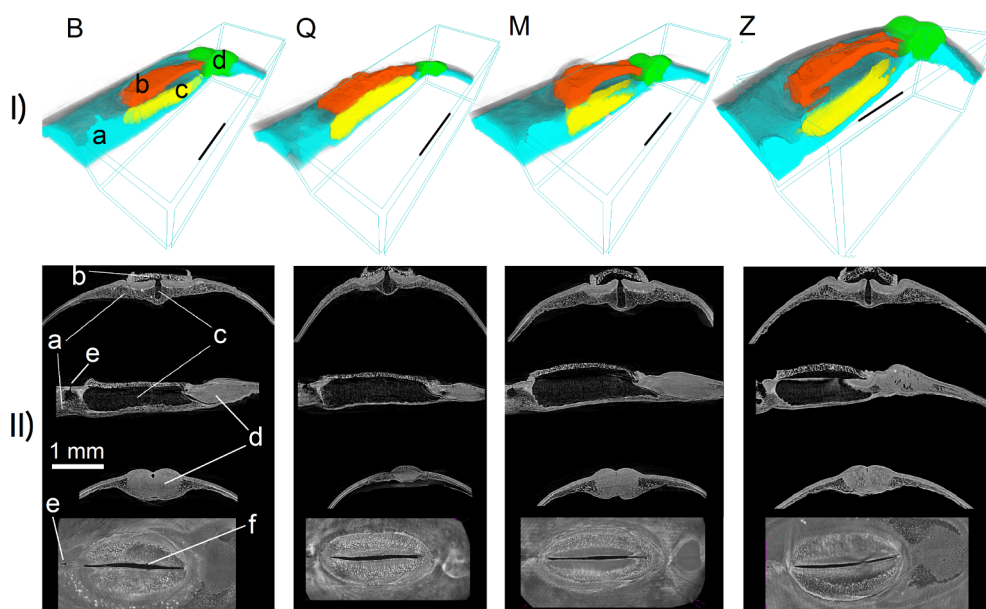


**Figure 1.** (I) Three-dimensional reconstructions of the hilum region and its parts, (II) Transversal and longitudinal sections of the hilum, transversal section of the strophiole and horizontal section of the hilum. (a) Vascular tissue, (b) funicular tissue, (c) tracheid bars, (d) strophiole, for the four bean landraces Butirro (B), Quarantino (Q), Mustacciello (M) and Zampognaro (Z). (e) micropyle groove, (f) hilar groove.

Quantification of volumetric and morphological traits was performed on the reconstructed images by applying an object-based image analysis (OBIA) approach. It allowed the determination of morphometry of the whole seeds and of the different seed parts, treated as isolated objects segmented from the image background, as described previously. This approach was applied using the software “Image Pro Premier 3D”.<sup>6</sup>

In particular, from the bulk seed scans, the volume, the surface area, the percent of internal free space, the sphericity and the Feret diameter ratio of the whole seed were determined for each seed. The percent of internal free space was determined from the ratio between the volume of the internal free space and the whole volume of each bean. The sphericity was calculated as 6 volumes of the object divided by the equivalent diameter and surface area of object. For perfectly spherical objects, this parameter equals 1; for all other shapes it is less than 1. The specific surface area was calculated from the ratio between surface area and volume of each seed. The equivalent diameter was calculated as the diameter of a sphere having the same volume of the seed.

From the single seed scans, the volumes of the different tissues of the hilum region (funicular tissue, vascular tissue, tracheid bars, strophiole) were determined after the image segmentation using the same software as above.

From the transversal sections of the hilum region the seed coat thickness was measured with digital micrometer. From the longitudinal sections of the hilum and the micropyle, the hilum groove area and the micropyle hole area were measured. These measurements were performed using the software “Image Pro Premier 3D”.

## 2.5. Hydration experiments

For the hydration measurements, 15 g of pre-selected grains (without any damage) of each landrace were placed, in three replicates, into beakers and soaked in 4 L of distilled water (to prevent water from being a limiting factor in the process) at  $25 \pm 1$  °C during the whole process. The initial moisture content  $M_0$  ranged between 8.2 %d.b. and 9.7 %d.b., in average, depending on the bean landrace (see Table 2). The moisture values are expressed as exceeding weight percent respect to dry basis (%d.b.). Bean dry weights were determined putting 15 g of beans for each landrace in oven at 103 °C for 72 h according to A.S.A.E. (2001). During the hydration process, the grains were periodically

drained (see Supplementary data sheet 2), superficially dried and weighted. Then, the grains were soaked again to continue the process. Three hours long hydration experiment was also performed sealing the bean seed coat except for the hilum region. A varnish (nail polish; L’Oréal, Paris) was used as covering sealant, similarly to Miano et al. (2016). This treatment allowed quantifying the initial contribution to the hydration due exclusively to the water entry across the hilum region.

### 2.5.1. Modeling of the hydration process

The bean hydration kinetics were modeled using Weibull distribution model:

$$M_t = M_0 - (M_0 - M_e) * (1 - \exp \left[ -\left( \frac{t}{\beta} \right)^\alpha \right])$$

where  $M_t$ ,  $M_0$  and  $M_e$  are the moisture contents at the time  $t$ , at the initial time 0 and at the equilibrium  $e$ , respectively. The parameter  $\alpha$  is a shape parameter and  $\beta$  is a scale parameter.

For that purpose, the dry basis moisture content of the grains ( $M$  % d.b.) versus the hydration time (min) was tabulated for each bean landrace. The data were fitted to the mathematical model with a confidence level of 95% using SigmaPlot software, version 13.0,<sup>7</sup> determining  $\alpha$ ,  $\beta$  and  $M_e$  as fitting parameters, fixing  $M_0$  and constraining the model to the average value of highest measured moisture content point obtained from the three replicated hydration experiments.

The goodness of fit of the model was evaluated by the  $R^2$  regression value and the root-mean-square error (RMSE) values.

The fitting of hydration process experimental data for coated seeds was performed using linear model, even if the latter did not provide always the best fitting, because in this case the priority was to compare trends by means of a single parameter.

## 2.6. Statistical analysis

Anova and LSD Fisher tests at a significance level of 0.05 were carried out to check differences in the results among the four considered bean landraces. Principal component analysis (PCA) was also performed for all provided data. Component/score biplot and Pearson correlation matrix with p-values evaluation have then been determined.

<sup>6</sup> <http://www.mediacy.com>.

<sup>7</sup> [www.systatsoftware.com](http://www.systatsoftware.com).

**Table 1**

Average values of the bean morphometric parameters and standard errors (in brackets) for the four bean landraces. Average values sharing a letter on a row are not significantly different (Fisher LSD method) at a  $P < 0.05$ .

		Butirro	Quarantino	Mustacciello	Zampognaro
Bulk seed scan	Bean volume (mm <sup>3</sup> )	264(6)b	238(5)c	401(11)a	277(5)b
	Specific surface area (mm <sup>2</sup> /mm <sup>3</sup> )	0.795(0.008)b	0.838(0.005)a	0.703(0.008)c	0.792(0.006)b
	Feret ratio	1.58(0.01)c	1.86(0.02)a	1.76(0.02)b	1.71(0.02)b
	Sphericity	0.960(0.001)a	0.937(0.002)c	0.944(0.002)b	0.943(0.002)b
	free space (%) <sup>*</sup>	9.5(0.6)ab	6.5(0.5)c	9(1.0)b	11.6(1.5)a
Single seed scan	Volumes (mm <sup>3</sup> )				
	Vascular tissue	1.8(0.32)a	0.95(0.1)b	1.98(0.08)a	1.96(0.15)a
	Funicular tissue	0.30(0.09)	0.15(0.04)	0.29(0.02)	0.26(0.02)
	Tracheid bars	0.068(0.003)b	0.095(0.008)a	0.109(0.007)a	0.095(0.008)a
	Strophiole	1.07(0.04)b	0.58(0.11)c	1.40(0.04)a	1.63(0.07)a
	Micropyle groove area (μm <sup>2</sup> )	4473(5 9 8)a	2975(1 7 5)ab	2703(1059)ab	2086(3 7 5)b
	Hilar groove area (mm <sup>2</sup> )	0.132(0.022)a	0.112(0.018)ab	0.106(0.002)ab	0.062(0.009)b
	Seed coat thickness (μm)	60.0(1.1)	59.3(4.7)	58.7(5.2)	57.3(0.7)

\* Calculated on a seed sample of 10 to 15 size depending from the landrace.

**Table 2**

Kinetic and statistical parameters (average values and standard errors in brackets) for the Weibull and linear models fitted to the hydration kinetics data of the four bean landraces. Column values sharing a letter are not significantly different (Fisher LSD method) at a  $P < 0.05$ .

Weibull						Linear		
	$\alpha$	$\beta$ (min)	$M_0$ (%d.b.)	$M_e$ (% d.b.)	$R^2$	RMSE	a (% d.b./min)	$R^2$
Butirro	1.34(0.02)c	372.1(3.9)c	9.7(0.5)	125.6(0.8)b	0.997	2.158	0.029(0.003)a	0.921
Quarantino	1.37(0.02)c	464.0(5.2)b	9.3(0.4)	119.3(1.0)c	0.997	2.008	0.012(0.002)b	0.835
Mustacciello	1.72(0.04)b	478.2(5.2)b	8.4(0.4)	127.8(1.0)b	0.997	2.382	0.014(0.001)b	0.922
Zampognaro	2.26(0.05)a	722.0(6.9)a	8.2(0.5)	133.0(1.0)a	0.998	1.915	0.002(0.0002)c	0.934

All above analyses were performed using the software SigmaPlot version 13.0<sup>7</sup>

### 3. Results

In the upper part of [Figure 1](#) is shown a three-dimensional representation of the different structures segmented in the hilum region (one replicate for each landrace is reported as an example). The images reported in the lower part of the [Figure 1](#) show how these structures appear in two-dimensional sections. Further views of such bean seed structures are reported in [Supplementary Figure 1](#), [Supplementary Figure 2](#) and [Supplementary Figure 3](#), and [Supplementary Video 1](#) and [2](#).

In [Table 1](#) are reported the average values of the morphometric parameters of the grains determined from the bulk seed scans for each landrace and the average volumes of the different structures of the hilum region obtained from the single seed scans. The areas of the hilum openings are also reported. The complete dataset of morphometric results is reported in [Supplementary data sheet 1](#). Details of the statistical results resumed in [Table 1](#) can be found in [Supplementary Tables](#) from 1 till 12.

[Figure 2](#) shows average bean moisture data measured during the hydration experiments and the curves obtained from the data fitted with Weibull model. In the box of [Figure 2](#) are shown the data and linear trends of the hydration experiments performed after waterproofing the seed coat except for the hilum region. In [Table 2](#), for all the landraces, are reported the Weibull model parameters describing the bean hydration kinetics and the linear model slope “a”, describing the velocity of water entry allowed only across the hilum region. All data of hydration tests are reported in [Supplementary Data sheet 2](#).

Butirro, Quarantino and Mustacciello had a shape of the hydration curve more similar to each other than Zampognaro (see [Figure 2](#)). This latter landrace showed a clear pseudo-sigmoidal hydration behavior, while the others had hydration curves closer to a downward concave shape (DCS). The shape  $\alpha$  and scale  $\beta$  parameters (see [Table 2](#)) resulted significantly highest in Zampognaro than Mustacciello, Butirro and

Quarantino. Butirro showed the significantly lowest  $\beta$  parameter value. All landraces were not significantly different in their initial moisture contents ( $M_0$ ). Zampognaro and Quarantino showed the significantly highest and lowest moisture contents ( $M_e$ ) at the equilibrium, respectively.

Slopes of the linear trends of the hydration data with waterproofed seed coat represent the averaged water entry velocity across the hilum. In particular, as reported in [Table 2](#), the significantly highest slope “a” was for Butirro, followed by Quarantino and Mustacciello, which did not result significantly different from each other, and by Zampognaro which had the significantly lowest “a” parameter. The same slope order can be observed for the not sealed beans in first 180 min, although less leaning. Details of the statistical results resumed in [Table 2](#) can be found in [Supplementary Tables](#) from 13 till 17.

In [Figure 3](#) is reported the score/loadings bi-plot from PCA of all obtained data that showed a significant difference at least between two landraces. First two components PC1 and PC2 explain more than 83% of variability.

Regarding the differences among the four landraces, it can be noticed that they are located in three different quadrants of the bi-plot. In particular, Butirro and Quarantino are the most different, while Mustacciello and Zampognaro are those more similar with respect to the set of the considered parameters. Feret ratio is strongly inversely correlated with PC2, thus Quarantino and Butirro are those having the most and least elongated shape, respectively. Mustacciello and Zampognaro have a similar intermediate shape. Parameter  $\alpha$  of Weibull hydration model is the best correlated with PC1, thus Butirro and Zampognaro are those exhibiting the largest difference with respect to this parameter.

[Figure 3](#) allows to recognize also an evident inverse correlation between hilar groove area and the scale parameter  $\beta$  of the Weibull hydration model, a strong correlation between moisture at equilibrium  $M_e$  and strophiole volume, and a good correlation between the micropyle groove area and the “a” parameter of the linear hydration model.

In detail, in [Table 3](#) are reported the Pearson correlation coefficients and the related p-values between all evaluated traits in PCA. In this



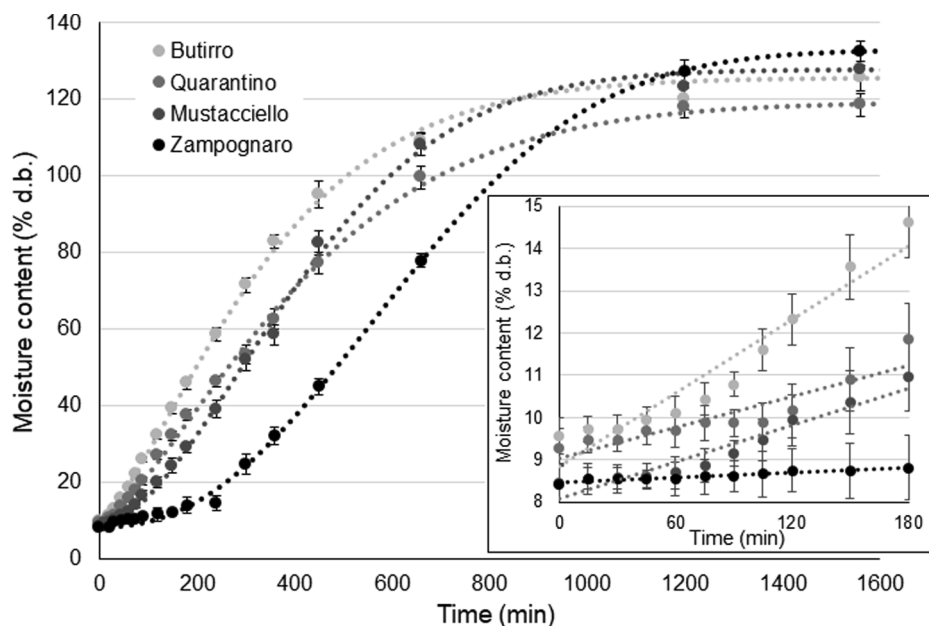


**Figure 2.** Hydration behavior of the four bean landraces. The dots are the experimental values averaged on the three replicates of the experiment and the vertical bars are the standard deviations; the fitting curves are obtained using the Weibull model. In the box are the data (the bars are the standard errors) and the linear trends of the hydration experiment performed waterproofing the seed coat except for the hilum region.

work, it was preliminarily decided to consider well-correlated the traits and parameters exhibiting Pearson coefficient values higher than 0.9 and with a p-value lower than 0.05, thus rejecting the hypothesis of lack of correlation with a significance level of 5%. Such coefficients are in bold character in Table 3.

Based on this premise, in addition to the good correlations

recognized in Figure 3, the free space percent resulted positively well-correlated with the water content value at the equilibrium  $M_e$  (0.970), while the hilar groove area resulted negatively well-correlated with the shape parameter  $\alpha$  ( $-0.971$ ). Among the morphometric parameters, resulted well-correlated the bean volume with the specific surface area ( $-0.985$ ), and the Feret ratio with the sphericity ( $-0.956$ ).  $\alpha$  and  $\beta$

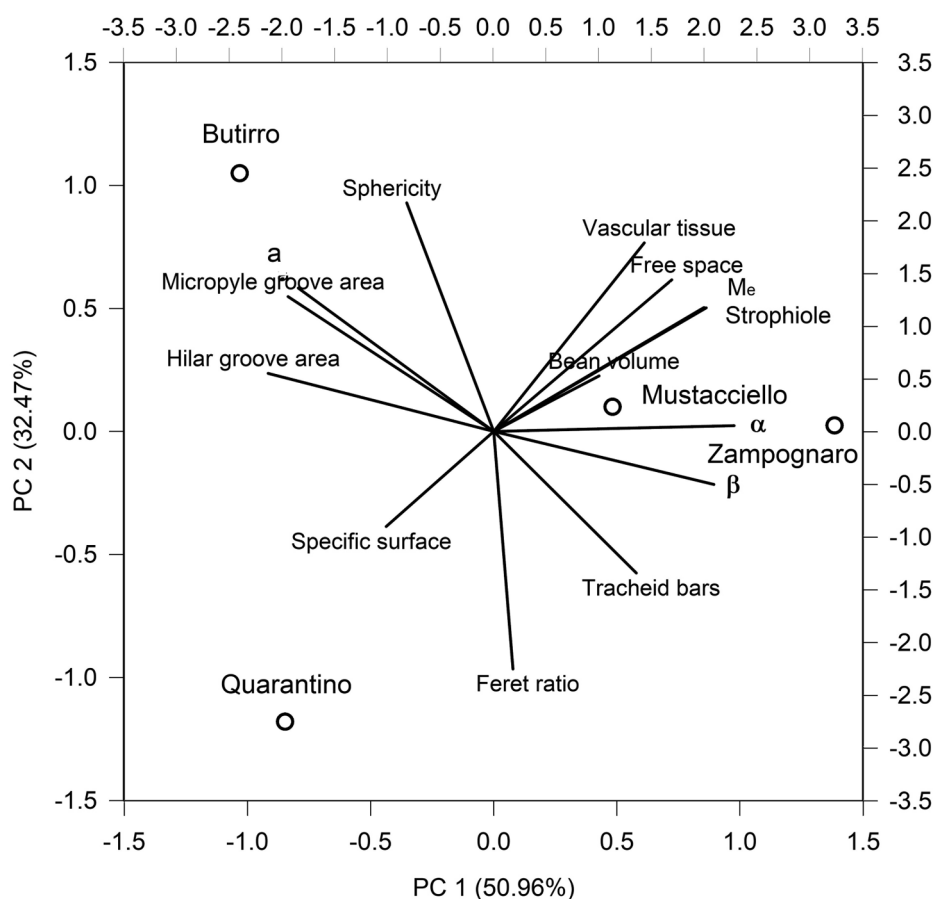


**Figure 3.** Score/loadings biplot from Principal Components Analysis (PCA) of all obtained data that exhibit at least one statistically significant difference among the four bean landraces. Circles are scores and refer to the primary axes. Loadings refer to the secondary axes.

**Table 3**

Pearson correlation coefficients (p-values below) among the morphometric traits of the bean hilum region and the hydration kinetic parameters.

	Specific surface	Feret ratio	Sphericity	Free space	Vascular tissue	Tracheid bars	Strophiole	Micropyle groove area	Hilar groove area	a	$\alpha$	$\beta$	$M_e$
Bean volume	<b>-0.985</b>	0.021	-0.035	0.181	0.609	0.623	0.534	-0.271	-0.030	-0.057	0.236	-0.006	0.375
	0.015	0.979	0.965	0.819	0.391	0.377	0.466	0.729	0.970	0.942	0.764	0.994	0.625
Specific surface		0.150	-0.120	-0.305	-0.726	-0.497	-0.618	0.185	0.0364	-0.020	-0.260	0.010	-0.471
		0.850	0.880	0.695	0.274	0.503	0.382	0.815	0.964	0.980	0.740	0.990	0.529
Feret ratio			<b>-0.956</b>	-0.590	-0.640	0.745	-0.393	-0.619	-0.143	-0.599	0.021	0.203	-0.441
			0.044	0.410	0.360	0.255	0.607	0.381	0.857	0.401	0.979	0.797	0.559
Sphericity				0.332	0.471	-0.802	0.150	0.813	0.427	0.808	-0.308	-0.481	0.179
				0.668	0.529	0.198	0.850	0.187	0.573	0.192	0.692	0.519	0.821
free space					0.851	-0.104	0.919	-0.266	-0.696	-0.282	0.795	0.645	<b>0.970</b>
					0.149	0.896	0.081	0.734	0.304	0.718	0.205	0.355	0.030
Vascular tissue						0.027	0.923	-0.099	-0.370	-0.004	0.570	0.304	0.887
Tracheid bars						0.973	0.077	0.901	0.630	0.996	0.430	0.696	0.113
							0.242	-0.823	-0.397	-0.695	0.428	0.416	0.130
							0.758	0.177	0.603	0.305	0.572	0.584	0.870
Strophiole								-0.448	-0.693	-0.383	0.841	0.642	<b>0.984</b>
								0.552	0.307	0.617	0.159	0.358	0.016
Micropyle groove area									0.830	<b>0.976</b>	-0.795	-0.849	-0.428
									0.170	0.024	0.205	0.151	0.572
Hilar groove area										0.878	<b>-0.971</b>	<b>-0.997</b>	-0.749
										0.122	0.029	0.003	0.251
a											-0.801	-0.904	-0.401
											0.203	0.0962	0.599
$\alpha$												<b>0.953</b>	0.869
												0.047	0.131
$\beta$													0.704
													0.299

parameters resulted positively well-correlated each other (0.953).

## 4. Discussion

### 4.1. Novelty of bean morphometric traits

Seed image analysis recently showed to be greatly useful for authentication and traceability of bean landraces (e.g., [Lo Bianco et al., 2015](#)). However, till now works aiming at morphometrically characterize the bean grains with images are based on the 2D image analysis approach ([Firatligil-Durmus, Sarka, Bubnik, Schejbal, & Kadlec, 2010](#); [Venora, Grillo, Ravalli, & Cremonini, 2009](#)) or extrapolated some 3D parameters using mathematical formulae ([Firatligil-Durmus et al., 2010](#)). Moreover, although [Gomes and Van Duijn \(2017\)](#) highlights the potential of the X-ray microCT in seed research and [Fiorani and Schurr \(2013\)](#) lists it among the techniques useful for seed phenotyping, to the best of our knowledge it has never been applied to bean grains. We here applied a twofold X-ray microCT approach to obtain an accurate 3D morphometric characterization of both, the whole bean grains and the internal structures of the hilum region ([Table 1](#)).

The approach we used for the whole bean grains characterization is similar to that [Guelpa et al. \(2016\)](#) used to characterize maize kernels and can be considered, likewise, a “high-throughput approach” to quickly phenotype a high number of seeds of different landraces of bean or other plant species. More precisely, we obtained morphometric results of about 70 bean grains in 3 h at 20  $\mu$ m image resolution.

The application of the single seed scanning approach for the 3D characterization of the hilum region structures, conversely, is absolutely inedited and has allowed recognizing very novel traits, as the different volumes ([Table 1](#)) and shapes ([Figure 1](#)) for these structures, which can be specific for each bean landrace (see also [Supplementary Figure 1](#) and [Supplementary Video 1 and 2](#)). In particular, the shape of the strophiole showed features peculiar for each studied landrace. Transversal sections in [Figure 1](#) allow to observe that the upper and lower surface of the strophiole of Mustacciello shows two “domes”, which are only on the upper surface in Butirro and Zampognaro.

Strophiole of Quarantino is the smallest and does not show any double protuberance. It is also possible to observe the presence of free space inside the strophiole of Zampognaro and of Butirro, less abundant in this latter. Moreover, from the transversal sections of the hilum it is possible to observe differences in the double palisade cell layer, which appears flat in Butirro and with an upward concavity for the other three landraces. These qualitative characteristics have been observed in all the three replicates ([Supplementary Figure 1](#) and [Supplementary Video 2](#)) analyzed for each landrace and could provide an useful contribution for identifying different bean genotypes, as stated by [Berrios et al. \(1998\)](#), and therefore for traceability of landraces.

### 4.2. Hydration kinetic modeling

Different mathematical models have been used to describe hydration kinetics of beans and predict the moisture content as a function of the process time ([Miano & Augusto, 2018](#)). Downward concave shape models (DCS) (e.g., [Peleg, 1988](#)) or the sigmoidal function (e.g., [Kaptso et al., 2008](#)) have been applied based on the permeability of the seed coat.

Although the experimental data for the four analyzed landraces, which started from the same (statistically) initial moisture content ([Miano et al., 2016](#)), showed different hydration behaviors, we chose the Weibull distribution model for all fittings. This quite simple and flexible model was found to be valuable in the description of the re-hydration kinetics of a variety of dried foods ([Zura et al., 2013](#); [Marabi, Livings, Jacobson, & Saguy, 2003](#); [Machado, Oliveira, & Cunha, 1999](#)). In particular, [López et al. \(2017\)](#) and [Ghafoor, Misra, Mahadevan, and Tiwari \(2014\)](#) observed that the Weibull model presented the best fit for the hydration kinetics data in different soaking treatments and for the majority of the studied bean varieties. Also in our work the values of the statistical parameters ( $R^2$  and RMSE) obtained from the data fitting (see [Table 2](#)) demonstrate the goodness of such model to describe the hydration behavior of all the studied landraces. The very different hydration behavior of Zampognaro was well described with the Weibull model by the very different  $\alpha$  and  $\beta$  parameters found. In fact, for  $\alpha$

equals one, the Weibull distribution reduces to a DCS, while for greater values provides a sigmoidal behavior and predicts the existence of a lag phase (Machado et al., 1999) whose extent is also related to the scale parameter  $\beta$ . This latter parameter physically is the time needed to accomplish approximately 63% of the moisture uptake process and is considered a general indicator of the rate of that process (Machado et al., 1999). Analogously, as sigmoidal bean hydration kinetics has been attributed to seed coat impermeability (e.g., Miano & Augusto, 2018), we suggest to use the shape parameter  $\alpha$  of the Weibull model as a trait for indicating the seed coat permeability of beans. Moreover, as Weibull is a sigmoidal model but not a strictly symmetrical one this allowed us to overcome the lack of fitting at the initial moisture content found by Miano et al. (2018) using Kapso's model.

#### 4.3. Role of hilum region structures in hydration behavior

Hypotheses on the role of hilum region structures in hydration behavior till now has been drawn by means of dye tracking experiments (e.g., Miano, García, & Augusto, 2015), using Magnetic Resonance microscopy (Mikac et al., 2015) or making SEM qualitative observations (Miano et al., 2018). We here used a quantitative approach based on the search of strong correlations between 3D measured morphometric traits and the hydration kinetics parameters.

Except for the good inverse correlations found between bean volume and its specific surface and between Feret ratio and Sphericity of bean seeds, which are due to the geometric definition of the two latter parameters, PCA and related calculation of Pearson coefficients reported in Table 3 allowed to enhance the understanding of the role of hilum region structures in hydration behavior.

Also Miano et al. (2018) tried to correlate different properties of beans with their hydration kinetics, but they only described qualitatively the microstructure of the beans and did not find correlations among microstructure of the beans and hydration kinetics parameters.

In the study of the hydration process of bean grains, a crucial issue to be addressed is the first entry of water into the grains. Waterproofing of some legume grain structures has already been performed in other researches in order to verify how grain hydration process changes (e.g., Miano et al., 2016). Mikac et al. (2015) used Magnetic Resonance microscopy to follow the water entry pathway. Some studies observed that there is a probability that the water enters through the micropyle or, to a lesser extent, the strophiole (Korban, Coyne, & Weihing, 1981; Agbo et al., 1987). However, most of the works attributed the main water entry to the hilum (Miano et al., 2016; Varriano-Marston & Jackson, 1981), whose area is larger than the micropyle and strophiole.

Our finding of very good correlation between the “a” parameter, obtained limiting water entry to the hilum region, and the micropyle groove area allows to precise that the micropyle opening is the hilum region structure which allows the first water entry in the bean seed.

The very good inverse correlation of hilar groove area with  $\alpha$  and  $\beta$  parameters indicates the role of hilar groove as a structure involved in the water entry during the entire bean hydration process. More precisely, the smaller is the hilar groove area the longer is the overall hydration process. To be noted the intrinsic correlation between  $\alpha$  and  $\beta$  parameters for bean hydration kinetics which is related to the above result.

Finally, two other measured traits exhibited significant positive correlation with the moisture  $M_e$  reached at equilibrium, namely, the bean free space percent and the strophiole volume. The first correlation confirms that during the hydration process the water is first distributed into the space between the internal face of the seed coat and then penetrate the cotyledons (Miano & Augusto, 2018). The correlation of the strophiole volume with the moisture content at equilibrium appears more difficult to interpret also considering that scientific literature for other legume grains reports this seed part mainly as a preferential water entry structure (e.g., Karaki, Watanabe, Kondo, & Koike, 2012; Kikuchi et al., 2006).

## 5. Conclusions

In this study, inedited 3D images of bean hilum region structures of four landraces have been provided and analyzed along with bean hydration data. Correlation between the obtained morphometric data and parameters of hydration kinetic models has been used as new investigation approach allowing to advance the understanding of the role of each single hilum region part in water uptake behavior. In particular the different roles of micropyle and hilum groove have been clarified, being the first involved in the very initial hydration stage, the second in the whole hydration process. Analysis of hydration kinetics has also led to consider the shape parameter  $\alpha$  of the Weibull model as a trait suitable for characterizing the seed coat permeability of beans. Moreover, the novel approach of internal structures imaging of beans has proved to be useful for bean landrace identification and authentication, when the more evident external traits are not sufficient for that purpose.

## CRedit authorship contribution statement

**Laura Gargiulo:** Investigation, Formal analysis, Visualization, Writing - original draft. **Giuseppe Sorrentino:** Resources. **Giacomo Mele:** Conceptualization, Methodology, Supervision, Writing - review & editing.

Declaration of Competing Interest

The authors declare that they have no known competing financial interests or personal relationships that could have appeared to influence the work reported in this paper.

## Acknowledgements

Thanks to Sabato Abbagnale, Silvia d'Ambra, Giulio Dubbioso and Antonio Prospero, stewards of biodiversity, for their kindly collaboration and Giuseppe Orefice of Slow Food Campania.

## Appendix A. Supplementary data

Supplementary data to this article can be found online at <https://doi.org/10.1016/j.foodres.2020.109211>.

## References

- Agbo, G. N., Hosfield, G. L., Uebersax, M. A., & Klomparsen, K. (1987). Seed microstructure and its relationship to water uptake in isogenic lines and a cultivar of dry beans (*Phaseolus vulgaris* L.). *Food Structure*, 6(1), 12.
- A. S. A. E. (2001). Moisture measurement-unground grain and seeds. In American Society of Agricultural Engineering Standard, 567–568.
- Berrios, J. D. J., Swanson, B. G., & Cheong, W. A. (1998). Structural characteristics of stored black beans (*Phaseolus vulgaris* L.). *Scanning*, 20, 410–417. <https://doi.org/10.1002/sca.1998.4950200507>.
- Chávez-Servia, J. L., Heredia-García, E., Mayek-Pérez, N., Aquino-Bolaños, E. N., Hernández-Delgado, S., & Carrillo-Rodríguez, J. C. (2016). Diversity of common bean (*Phaseolus vulgaris* L.) landraces and the nutritional value of their grains. In A. Goyal (Ed.), *Grain LegumesIntechOpen* chapter 1. <https://doi.org/10.5772/63439>.
- Fiorani, F., & Schurr, U. (2013). Future Scenarios for plant phenotyping. *Annual Review of Plant Biology*, 64, 267–291. <https://doi.org/10.1146/annurev-arplant-050312-120137>.
- Firatligil-Durmaz, E., Sarka, E., Bubnik, Z., Schejbal, M., & Kadlec, P. (2010). Size properties of legume seeds of different varieties using image analysis. *Journal of Food Engineering*, 99(4), 445–451.
- Gargiulo, L., Grimberg, Á., Repo-Carrasco-Valencia, R., Carlsson, A. S., & Mele, G. (2019). Morpho-densitometric traits for quinoa (*Chenopodium quinoa* Willd.) seed phenotyping by two X-ray micro-CT scanning approaches. 102829 *Journal of Cereal Science*, 90. <https://doi.org/10.1016/j.jcs.2019.102829>.
- Ghafoor, M., Misra, N. N., Mahadevan, K., & Tiwari, B. K. (2014). Ultrasound assisted hydration of navy beans (*Phaseolus vulgaris*). *Ultrasonics Sonochemistry*, 21, 409–414. <https://doi.org/10.1016/j.ultsonch.2013.05.016>.
- Gomes, F. G., & Van Duijn, B. (2017). Three-dimensional (3-D) X-ray Imaging for Seed Analysis. *Seed Testing International*, 153, 45–50.
- Guelpa, A., du Plessis, A., & Manley, M. (2016). A high-throughput X-ray micro-computed tomography ( $\mu$ CT) approach for measuring single kernel maize (*Zea mays* L.) volumes and densities. *Journal of Cereal Science*, 69, 321–328. <https://doi.org/10.1016/J.JCS.2016.04.009>.
- Gustin, J. L., Jackson, S., Williams, C., Patel, A., Armstrong, P., Peter, G. F., et al. (2013).

- Analysis of maize (*Zea mays*) kernel density and volume using microcomputed tomography and single-kernel near-infrared spectroscopy. *Journal of Agricultural and Food Chemistry*, 61, 10872–10880. <https://doi.org/10.1021/jf403790v>.
- Kaptsio, K. G., Njintang, Y. N., Komnek, A. E., Hounhouigan, J., Scher, J., & Mbofung, C. M. F. (2008). Physical properties and rehydration kinetics of two varieties of cowpea (*Vigna unguiculata*) and bambara groundnuts (*Voandzeia subterranea*) seeds. *Journal of Food Engineering*, 86, 91–99. <https://doi.org/10.1016/J.JFOODENG.2007.09.014>.
- Karaki, T., Watanabe, Y., Kondo, T., & Koike, T. (2012). Strophiole of seeds of the black locust acts as a water gap. *Plant Species Biology*, 27, 226–232. <https://doi.org/10.1111/j.1442-1984.2011.00343.x>.
- Khattab, R. Y., & Arntfield, S. D. (2009). Nutritional quality of legume seeds as affected by some physical treatments 2. Antinutritional factors. *LWT - Food Science and Technology*, 42, 1113–1118. <https://doi.org/10.1016/J.LWT.2009.02.004>.
- Kikuchi, K., Koizumi, M., Ishida, N., & Kano, H. (2006). Water uptake by dry beans observed by micro-magnetic resonance imaging. *Annals of Botany*, 98, 545–553. <https://doi.org/10.1093/aob/mcl145>.
- Korban, S., Coyne, D., & Weihing, J. (1981). Rate of water uptake and sites of water entry in seeds of different cultivars of dry bean. *HortScience*, 16, 545–546.
- Kotue, T. C., Marlyne, J. M., Wirba, L. Y., Amalene, S. R. H., Nkenmeni, D. C., Kwumgoin, I., et al. (2018). Nutritional properties and nutrients chemical analysis of common beans seed. *MOJ Biology and Medicine*, 3(3), 41–47. <https://doi.org/10.15406/mojbm.2018.03.00074>.
- Lo Bianco, M., Grillo, O., Cremonini, R., Sarigu, M., & Venora, G. (2015). Characterisation of Italian bean landraces (*Phaseolus vulgaris* L.) using seed image analysis and texture descriptors. *Australian Journal of Crop Science*, 9, 1022–1034. <https://doi.org/10.1016/j.scienta.2009.03.014>.
- López, L. R. L., Ulloa, J. A., Ulloa, P. R., Ramírez, J. C. R., Carrillo, Y. S., & Ramos, A. Q. (2017). Modelling of hydration of bean (*Phaseolus vulgaris*): Effect of the low-frequency ultrasound. *Italian Journal of Food Science*, 29, 288–301. <https://doi.org/10.14674/1120-1770/ijfs.v686>.
- Machado, M. F., Oliveira, F. A. R., & Cunha, L. M. (1999). Effect of milk fat and total solids concentration on the kinetics of moisture uptake by ready-to-eat breakfast cereal. *International Journal of Food Science & Technology*, 34, 47–57. <https://doi.org/10.1046/j.1365-2621.1999.00238.x>.
- Marabi, A., Livings, S., Jacobson, M., & Saguy, I. S. (2003). Normalized Weibull distribution for modelling rehydration of food particulates. *European Food Research and Technology*, 217, 311–318. <https://doi.org/10.1007/s00217-003-0719-y>.
- Martínez-Manrique, E., Jacinto-Hernández, C., Garza-García, R., Campos, A., Moreno, E., & Bernal-Lugo, I. (2011). Enzymatic changes in pectic polysaccharides related to the beneficial effect of soaking on bean cooking time. *Journal of the Science of Food and Agriculture*, 91, 2394–2398. <https://doi.org/10.1002/jsfa.4474>.
- Miano, A. C., & Augusto, P. E. D. (2018). The hydration of grains: A critical review from description of phenomena to process improvements. *Comprehensive Reviews in Food Science and Food Safety*, 17, 352–370. <https://doi.org/10.1111/1541-4337.12328>.
- Miano, A. C., Saldaña, E., Campestrini, L. H., Chiorato, A. F., & Augusto, P. E. D. (2018). Correlating the properties of different carioca bean cultivars (*Phaseolus vulgaris*) with their hydration kinetics. *Food Research International*, 107, 182–194. <https://doi.org/10.1016/j.foodres.2018.02.030>.
- Miano, A. C., Pereira, J. da C., Castanha, N., Júnior, M. D. da M., & Augusto, P. E. D. (2016). Enhancing mung bean hydration using the ultrasound technology: description of mechanisms and impact on its germination and main components. *Scientific Reports*, 6, 38996. <https://doi.org/10.1038/srep38996>.
- Miano, A. C., García, J. A., & Augusto, P. E. D. (2015). Correlation between morphology, hydration kinetics and mathematical models on Andean lupin (*Lupinus mutabilis* Sweet) grains. *LWT - Food Science and Technology*, 61, 290–298. <https://doi.org/10.1016/j.lwt.2014.12.032>.
- Mikac, U., Sepe, A., & Serša, I. (2015). MR microscopy for noninvasive detection of water distribution during soaking and cooking in the common bean. *Magnetic Resonance Imaging*, 33, 336–345. <https://doi.org/10.1016/J.MRI.2014.12.001>.
- Peleg, M. (1988). An empirical model for the description of moisture sorption curves. *Journal of Food Science*, 53, 1216–1217. <https://doi.org/10.1111/j.1365-2621.1988.tb13565.x>.
- Piergiovanni, A. R., & Lioi, L. (2010). Italian common bean landraces: History, genetic diversity and seed quality. *Diversity*, 2, 837–862. <https://doi.org/10.3390/d2060837>.
- Schoeman, L., Williams, P., du Plessis, A., & Manley, M. (2016). X-ray micro-computed tomography (μCT) for non-destructive characterisation of food microstructure. *Trends in Food Science & Technology*, 47, 10–24. <https://doi.org/10.1016/J.TIFS.2015.10.016>.
- Siano, F., Sorrentino, G., Riccardi, M., De Cunzio, F., Orefice, G., & Volpe, M. G. (2018). Chemical, nutritional, and spectroscopic characterization of typical ecotypes of Mediterranean area beans. *European Food Research and Technology*, 244(5), 795–804. <https://doi.org/10.1007/s00217-017-3004-1>.
- Varriano-Marston, E., & Jackson, G. M. (1981). Hard-to-Cook phenomenon in beans: Structural changes during storage and imbibition. *Journal of Food Science*, 46, 1379–1385. <https://doi.org/10.1111/j.1365-2621.1981.tb04179.x>.
- Venora, G., Grillo, O., Ravalli, C., & Cremonini, R. (2009). Identification of Italian landraces of bean (*Phaseolus vulgaris* L.) using an image analysis system. *Scientia Horticulturae*, 121(4), 410–418.
- Veteläinen, M., Negri, V., & Maxted N. (2009). European landraces on farm conservation, management and use. Bioversity Technical Bulletin No. 15. Bioversity International, Rome, Italy.
- Xiao, S., Bresler, Y., & Munson, D. C. (2003). Fast Feldkamp algorithm for cone-beam computer tomography. Proceedings International Conference on Image Processing (Cat. No.03CH37429), Barcelona, Spain, 819–822. <https://doi.org/10.1109/ICIP.2003.1246806>.
- Zura, L., Uribe, E., Lemus-Mondaca, R., Saavedra-Torrico, J., Vega-Gálvez, A., & Di Scala, K. (2013). Rehydration capacity of Chilean papaya (*Vasconcellea pubescens*): Effect of process temperature on kinetic parameters and functional properties. *Food and Bioprocess Technology*, 6, 844–850. <https://doi.org/10.1007/s11947-011-0677-5>.